Analytical expression for the RKKY interaction in doped graphene

M. Sherafati and S. Satpathy

Phys. Rev. B **84**, 125416 — Published 7 September 2011

DOI: 10.1103/PhysRevB.84.125416

Analytical Expression for the RKKY Interaction in Doped Graphene

M. Sherafati and S. Satpathy
Department of Physics & Astronomy, University of Missouri, Columbia, MO 65211

(Dated: August 5, 2011)

We obtain an analytical expression for the Ruderman-Kittel-Kasuya-Yosida (RKKY) interaction J in electron or hole doped graphene for linear Dirac bands, extending our earlier results for the undoped case.[1] The results agree very well with the numerical calculations for the full tight-binding band structure in the regime where the linear band structure is valid. The analytical result, expressed in terms of the Meijer G-function, consists of the product of two oscillatory terms, one coming from the interference between the two Dirac cones and the second coming from the finite size of the Fermi surface. For large distances, the Meijer G-function behaves as a sinusoidal term, leading to the result $J \sim R^{-2} k_F \sin(2k_F R)\{1+\cos[(\vec{K}-\vec{K}').\vec{R}]\}$ for moments located on the same sublattice. The R^{-2} dependence, which is the same for the standard two-dimensional electron gas, is universal irrespective of the sublattice location and the distance direction of the two moments except when $k_F = 0$ (undoped case), where it reverts to the R^{-3} dependence. These results correct several inconsistencies found in the literature.

PACS numbers: 75.30.Hx; 75.10.Lp; 75.20.Hr

I. INTRODUCTION

The Ruderman-Kittel-Kasuya-Yosida (RKKY) interaction,[2] which measures the coupling between two magnetic moments mediated by a background of electrons, is an important characteristic of the electron system and a fundamental interaction responsible for magnetic ordering in spin glasses and alloys. It has been extensively studied for the electron gas in one[3], two[4], or three dimensions.

Even though graphene is a two-dimensional (2D) system, there are two important differences from the standard 2D electron gas, viz., the linear band structure and the existence of two Dirac cones in the Brillouin zone (BZ). Therefore, for describing the RKKY interaction in graphene, these two unique features must be correctly taken into account. The RKKY interaction in graphene has already been studied by many authors both for the doped and the undoped case[5–13]. However, the results differ from one another, either in the power-law decay, or in the oscillatory behavior in the long-distance limit, or sometimes even in the sign of the interaction, viz., ferromagnetic (FM) or anti-ferromagnetic (AFM). In an important piece of work on undoped graphene, Saremi[5] showed that particle-hole symmetry in a bipartite lattice leads to definite signs of the RKKY interaction, viz., FM for moments on the same sublattice and AFM for moments on the opposite sublattices. The symmetry exists if the weak beyond-nearest-neighbor interactions are neglected. Nevertheless, the interference term from the two Dirac cones is either computed incompletely or completely unnoticed in the mainstream literature, the fact that was highlighted in our previous work for the undoped case.[1] Moreover, due to the similarity between the RKKY interaction and the Friedel oscillations, the same inconsistencies exist in the literature for the Friedel oscillations as well.[12–15]

In this paper, we derive analytical expressions for the RKKY interaction for the linear band model for the doped case, extending our earlier work for the undoped case,[1] and compare the analytical results with the numerical results obtained using the tight-binding band structure.

The analytical results, summarized in Table I, are expressed in terms of the Meijer G-function, whose long distance behavior is sinusoidal. We find that the analytical results in the linear band approximation may be expressed as a product of the J for the undoped case, which is obviously independent of the Fermi momentum k_F but depends on the momentum difference of the two Dirac points, $\vec{K}-\vec{K}'$, and a second factor coming from the doped electrons that depends on k_F. This second factor does go to one, as it must, in the limit of $k_F \to 0$, so that the results for the undoped case are correctly reproduced from the general results. Each of the two characteristic momenta, viz., k_F and $\vec{K}-\vec{K}'$, produces an oscillatory factor of its own, leading to unusual features not found in the standard 2D electron gas, e.g., the beating of the RKKY interaction in certain cases, which can be tuned by a gate voltage. The linear-band and the tight-binding results agree quite well in the cases where k_F lies in the linear regime ($|E_F| \lesssim t/3$).

II. MODEL AND THE METHOD

We consider the nearest-neighbor tight-binding Hamiltonian for the π-electrons in graphene including the contact interaction with two localized magnetic moments

$$\mathcal{H} = \mathcal{H}_0 + \mathcal{H}_{\rm int}, \tag{1}$$

where $\mathcal{H}_0 = -t\sum_{\langle ij\rangle\sigma} c^\dagger_{i\sigma}c_{j\sigma} + H.c.$ is the tight-binding Hamiltonian, $\langle ij\rangle$ denotes summation over distinct pairs of nearest neighbors, $t \approx 2.56$ eV,[17] σ is the spin index, and the interaction term between the localized spins $\vec{S}_p$

TABLE I: Summary of the RKKY interaction in graphene for both the doped ($k_F \neq 0$) and the undoped case ($k_F = 0$), given as a product of the terms: $J_{\alpha\beta} = \alpha_C \alpha_D \alpha_F$. The long-distance behavior is obtained by replacing α_F with α'_F. Here $C \equiv 9\lambda^2\hbar^2/(256\pi t)$, $C' \equiv -\lambda'^2 V^2 m^*/8(N\pi\hbar)^2$, $x_D = (\vec{K} - \vec{K'}) \cdot \vec{R}$, $x_F = k_F R$, θ_R is the angle of the position vector $\vec{R}$ made with $\vec{K'} - \vec{K}$ direction, where $\vec{K'}$ and $\vec{K}$ are two adjacent Dirac points in the BZ. The results for the standard two-dimensional electron gas (2DEG)[4] are also shown, where we have rederived the long-distance behavior.

Sublattices α, β	k_F	α_C Prefactor	α_D Dirac-cone factor	α_F Fermi factor	α'_F Long-distance behavior of α_F
AA	0	$-C(R/a)^{-3}$	$1+\cos x_D$	1	1
AA	k_F	$-C(R/a)^{-3}$	$1+\cos x_D$	$1+8\pi^{-1/2}x_F M(x_F)$	$\pi^{-1}[2\cos(2x_F)+8x_F\sin(2x_F)]$
AB	0	$3C(R/a)^{-3}$	$1+\cos(x_D+\pi-2\theta_R)$	1	1
AB	k_F	$3C(R/a)^{-3}$	$1+\cos(x_D+\pi-2\theta_R)$	$1-8(9\pi)^{-1/2}x_F M'(x_F)$	$(3\pi)^{-1}[10\cos(2x_F)+8x_F\sin(2x_F)]$
2DEG	k_F	$C'R^{-2}$	1	$x_F^2[J_0(x_F)Y_0(x_F)+J_1(x_F)Y_1(x_F)]$	$(4\pi x_F)^{-1}[\cos(2x_F)-4x_F\sin(2x_F)]$

and the itinerant electron spins $\vec{s}_p$ is given by

$$\mathcal{H}_{\rm int} = -\lambda(\vec{S}_1 \cdot \vec{s}_1 + \vec{S}_2 \cdot \vec{s}_2). \tag{2}$$

In the linear response theory, the interaction energy may be written in the Heisenberg form

$$E(\vec{R}) = J_{\alpha\beta}(\vec{R})\vec{S}_1 \cdot \vec{S}_2, \tag{3}$$

where the sublattice indices and the positions of the two moments are $(\alpha, 0)$ and $(\beta, \vec{R})$, and their RKKY interaction (exchange integral) is given by

$$J_{\alpha\beta}(\vec{R}) = \frac{\lambda^2\hbar^2}{4}\chi_{\alpha\beta}(0,\vec{R}), \tag{4}$$

where the sublattice susceptibility is

$$\chi_{\alpha\beta}(\vec{r},\vec{r'}) \equiv \delta n_\alpha(\vec{r})/\delta V_\beta(\vec{r'}). \tag{5}$$

Here $\vec{R}$ denotes the position of the atom, in contact with the impurity, and *not* the position of the cell in which it is located; they differ by the basis vector of the atom in the unit cell.

Note from Eq. (5) that the Friedel oscillations in graphene[12–15], $\delta n_\alpha(\vec{r})$ in the charge density induced by a δ-function potential, is proportional to $J_{\alpha\beta}$ as well.

Using the Dyson equation, the sublattice susceptibility can be written in terms of the unperturbed Green's function to yield

$$\chi_{\alpha\beta}(0,\vec{R}) = -\frac{2}{\pi}\int_{-\infty}^{E_F} dE\ {\rm Im}[G^0_{\alpha\beta}(0,\vec{R},E)G^0_{\beta\alpha}(\vec{R},0,E)]. \tag{6}$$

To evaluate the integral, we need to compute the unperturbed real-space Green's functions for graphene. We calculate these analytically for the linear bands and numerically for the tight-binding bands by direct integration,

$$G^0_{\alpha\beta}(\vec{R},0,E) = \frac{1}{\Omega_{BZ}}\int d^2k e^{i\vec{k}\cdot\vec{R}} G^0_{\alpha\beta}(\vec{k},E), \tag{7}$$

of the momentum-space Green's function

$$G^0_{\alpha\beta}(\vec{k},E) = \frac{E+i\eta+\mathcal{H}_{\vec{k}}}{(E+i\eta)^2-|f(\vec{k})|^2} \tag{8}$$

over the graphene Brillouin zone with area Ω_{BZ}. Here $\mathcal{H}_{\vec{k}} = \begin{pmatrix} 0 & f(\vec{k}) \\ f^*(\vec{k}) & 0 \end{pmatrix}$ is the graphene tight-binding Hamiltonian in the momentum space and the Bloch sum $f(\vec{k}) = -t\ (e^{i\vec{k}\cdot\vec{d}_1} + e^{i\vec{k}\cdot\vec{d}_2} + e^{i\vec{k}\cdot\vec{d}_3})$, where $\vec{d}_1$, $\vec{d}_2$ and $\vec{d}_3$ are the three nearest-neighbor position vectors.

A. Moments on the same sublattice

Using methods discussed in our previous work[1], the Green's functions as well as the susceptibility can be evaluated both for the linear-band approximation and for the full tight-binding bands. For the linear-band case and for moments on the same sublattice, the result is

$$\chi_{AA}(0,\vec{R}) = I_{AA}(R) \times \{1+\cos[(\vec{K}-\vec{K'})\cdot\vec{R}]\}, \tag{9}$$

where

$$I_{AA}(R) = -\frac{4}{\pi}\int_{-\infty}^{E_F} dE\ {\rm Im}\ [g_{AA}(R,E)]^2, \tag{10}$$

$g_{AA}(R,E) = -2\pi E v_F^{-2}\Omega_{BZ}^{-1}K_0(-iER/v_F)$, K_0 is the modified Bessel function of the second kind, $v_F = 3ta/2$ is the Fermi velocity, and a is the carbon-carbon bond length. Now we split the integral in Eq. (10) into two parts, viz., $\int_{-\infty}^{E_F} = \int_{-\infty}^{0} + \int_0^{E_F}$, where the first term accounts for the valance electrons (undoped case) and the second for the conduction electrons, so that

$$I_{AA}(R) = \frac{8\pi^3}{\Omega_{BZ}^2 v_F}R^{-3}[I_0 + \int_0^{k_F R} dz\ z^2 J_0(z)Y_0(z)], \tag{11}$$

where $I_0 = -\int_0^\infty dy\ y^2 J_0(y)Y_0(y) = -1/16$,[1,5] $y = -ER/v_F$ for the valance band ($E < 0$), $z = ER/v_F$

for the conduction band ($E > 0$) and J_0 and Y_0 are the Bessel and Neumann functions with real arguments and k_F is the Fermi momentum.

The remaining integral in Eq. (11) may be expressed in terms of the Meijer G-functions. The product of the Bessel and the Neumann functions can be written as

$$z^{\mu} J_{\nu}(z) Y_{\nu}(z) = -\frac{1}{\sqrt{\pi}} G^{2,0}_{1,3}\left(\begin{matrix} \frac{\mu+1}{2} \\ \frac{\mu}{2}, \frac{\mu}{2}+\nu, \frac{\mu}{2}-\nu \end{matrix} \middle| \, z^2 \right), \tag{12}$$

and using the integral tables[21] along with $\mu = 2$, $\nu = 0$, and the new variable $x = z^2 (k_F R)^{-2}$, the result is

$$\int_0^{k_F R} dz \; z^2 J_0(z) Y_0(z) = -\frac{k_F R}{2\sqrt{\pi}} \int_0^1 dx \; x^{-1/2} \times G^{2,0}_{1,3}\left(\begin{matrix} \frac{3}{2} \\ 1, 1, 1 \end{matrix} \middle| \, k_F^2 R^2 x \right) = -\frac{k_F R}{2\sqrt{\pi}} M(k_F R), \tag{13}$$

where

$$M(k_F R) = G^{2,1}_{2,4}\left(\begin{matrix} \frac{1}{2}, \frac{3}{2} \\ 1, 1, 1, \frac{-1}{2} \end{matrix} \middle| \, k_F^2 R^2 \right) \tag{14}$$

is a short-hand notation for the Meijer G-function. Plugging Eqs. (13), (11) and (9) into Eq. (4), we find the exact analytical RKKY interaction J, valid for all distances and for the linear bands, viz.,

$$J_{AA}(\vec{R}) = J^0_{AA}(\vec{R}) \; [1 + \frac{8 k_F R}{\sqrt{\pi}} M(k_F R)], \tag{15}$$

where

$$J^0_{AA}(\vec{R}) = -\frac{C a^3}{R^3} \times \{1 + \cos[(\vec{K} - \vec{K}') \cdot \vec{R}]\} \tag{16}$$

is the undoped exchange interaction with $C \equiv 9\lambda^2 \hbar^2/(256\pi t)$. The only approximation used here was to extend the linearity of the Dirac bands to infinity (infinite momentum cutoff); however, this approximation is in good agreement with the numerical full-band tight-binding calculations, both for the undoped case[1] and for the doped case if k_F is small [Fig. (1)]. It is not surprising that the Meijer G-functions also appear in the RKKY interaction for the topological insulators which contain a linear part in the band dispersion just like graphene.[16]

Note that in the expression for the RKKY interaction Eq. (15) the Fermi momentum term in the square bracket depends only on the magnitude of the distance, R, while the Dirac-cones term in $J^0_{AA}(\vec{R})$ depends on its direction as well, which makes the interaction direction-dependent. Here $\vec{K}$ and $\vec{K}'$ are any two adjacent Dirac points in the BZ. It is easy to see that while the oscillatory factor $1 + \cos((\vec{K} - \vec{K}') \cdot \vec{R})$ repeats in triplets as 2, 1/2, 1/2, ... with distance R along the zigzag direction, it is always two for the armchair direction, so that J_{AA} changes smoothly along the armchair direction but not for the zigzag direction [Fig. (2)].

One is often interested in the long-distance behavior of the RKKY interaction and this may be obtained from

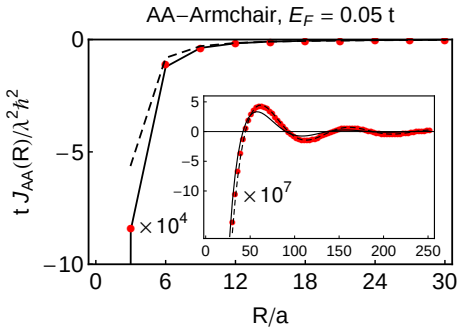

FIG. 1: (Color online) RKKY interaction J_{AA} obtained for the tight-binding bands (solid line), compared to the RKKY expression involving the Meijer G-function Eq. (15) (red dots) and its long-distance limit Eq. (19) (dashed line).

the asymptotic behavior of the Meijer G-function $M(x)$. We find using standard tables[21] that

$$\lim_{x \to 0} M(x) = \frac{4x^2[1 - 3\gamma - 3\ln(x/2)]}{9\sqrt{\pi}} \tag{17}$$

$$\lim_{x \to \infty} M(x) = -\frac{\pi - 2\cos(2x) - 8x\sin(2x)}{8\sqrt{\pi} x}, \tag{18}$$

where $\gamma \approx 0.577$ is the Euler-Mascheroni constant. These functions are plotted in Fig. (3). We note that with this asymptotic dependence, the square bracket in Eq. (15) becomes one for $k_F = 0$, so that the RKKY interaction becomes the same as for the undoped case as it must.

Contrary to $J^0_{AA}(\vec{R})$ that always shows ferromagnetic coupling for the moments on the same sublattices owing to the particle-hole symmetry[5], the oscillatory behavior of $M(k_F R)$ leads to the oscillations of J_{AA} between ferromagnetic and anti-ferromagnetic interactions. From Eqs. (18) and (15), we obtain the long-distance behavior

$$\lim_{k_F R \to \infty} J_{AA}(\vec{R}) = \frac{J^0_{AA}(\vec{R})}{\pi} [2\cos(2x_F) + 8x_F \sin(2x_F)], \tag{19}$$

where $x_F = k_F R$.

Note that the distance dependence is R^{-2} if k_F is non-zero, i. e., the same as for the ordinary 2D electron gas[4]. If $k_F = 0$, the RKKY interaction reverts to the undoped case as seen from Eqs. (15) and (17), so that the distance dependence is now R^{-3}.

It is worth mentioning that the correct result for $k_F R \gg 1$ can only be found by evaluating the Meijer G-function for large arguments and not just by replacing the Bessel functions in Eq. (13) by their large-argument ($z \gg |\nu^2 - 1/4|$) limits, viz., $J_\nu(z) \approx 2^{1/2}(\pi z)^{-1/2} \cos(z - \nu\pi/2 - \pi/4)$ and $Y_\nu(z) \approx 2^{1/2}(\pi z)^{-1/2} \sin(z - \nu\pi/2 - \pi/4)$. The latter approach happens to lead to the same functional form as in Eq. (19) but with incorrect coefficients because of the error made in the small $k_F R$ contribution to the integral in Eq. (13).

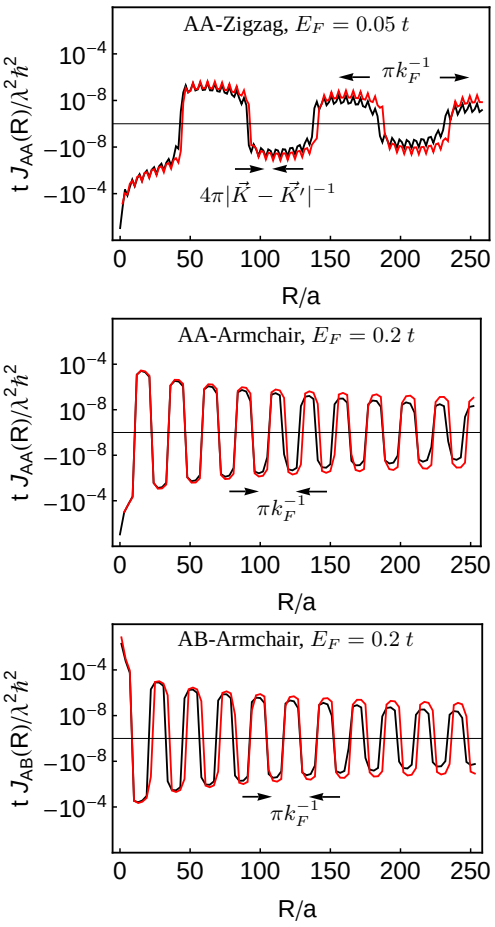

FIG. 2: (Color online) RKKY interaction for several cases. Black solid lines are the numerical results for the full tight-binding band structure, while the red lines indicate the analytical results, Eqs. (15) and (25), for the linear bands.

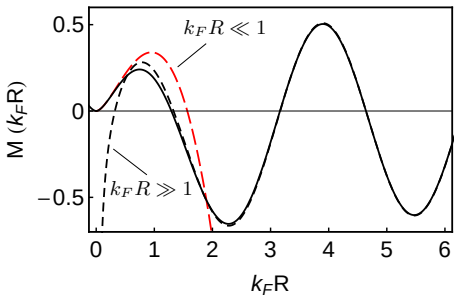

FIG. 3: (Color online) The Meijer G-function as a function of $k_F R$ (black solid line) versus its asymptotic expansions (Eqs. 17 and 18).

There is no such problem if $k_F R \ll 1$ and the short-range results can be found by using the asymptotic expansion of the Meijer G-function, Eq. (17), or by using the small argument $[0 < z \ll \sqrt{\nu+1}]$ expansions, viz.,

$$J_\nu(z) \approx \frac{1}{\Gamma(\nu+1)}\left(\frac{z}{2}\right)^\nu \tag{20}$$

$$Y_\nu(z) \approx \begin{cases} \frac{2}{\pi}\left[\ln(z/2)+\gamma\right] & \text{if } \nu = 0 \\ -\frac{\Gamma(\nu)}{\pi}\left(\frac{2}{z}\right)^\nu & \text{if } \nu > 0. \end{cases}$$

The result in this limit is

$$\lim_{k_F R\to 0} \quad J_{AA}(\vec{R}) = J^0_{AA}(\vec{R}) \times \{1 + \frac{32(k_F R)^3}{9\pi}[1 - 3\gamma - 3\ln(k_F R/2)]\}. \tag{21}$$

B. Moments on the opposite sublattices

For moments located on two different sublattices, we proceed as before to obtain the susceptibility[1]

$$\chi_{AB}(0,\vec{R}) = I_{AB}(R) \times \{1 + \cos[(\vec{K} - \vec{K}')\cdot\vec{R} + \pi - 2\theta_R]\}, \tag{22}$$

where $I_{AB}(R) = \frac{4}{\pi}\int_{-\infty}^{E_F} dE\ \ \mathrm{Im}\ [g_{AB}(R,E)]^2$ with $g_{AB}(R,E) = -2\pi E v_F^{-2}\Omega_{BZ}^{-1} K_1(-iER/v_F)$ and θ_R is the angle of the position vector $\vec{R}$ with respect to the $\vec{K}' - \vec{K}$ direction. Expanding the modified Bessel function K_1, the integral becomes

$$I_{AB}(R) = \frac{8\pi^3 R^{-3}}{\Omega_{BZ}^2 v_F}[I'_0 + \int_0^{k_F R} dz\ z^2 J_1(z) Y_1(z)], \tag{23}$$

where $I'_0 = -\int_0^\infty dy\ y^2 J_1(y) Y_1(y) = 3/16$[1,5] is the contribution from the undoped part and the remaining integral can again be expressed in terms of the Meijer G-function

$$\int_0^{k_F R} dz\ z^2 J_1(z) Y_1(z) = -\frac{k_F R}{2\sqrt{\pi}} M'(k_F R). \tag{24}$$

This leads to the final result

$$J_{AB}(\vec{R}) = J^0_{AB}(\vec{R})\ [1 - \frac{8 k_F R}{3\sqrt{\pi}} M'(k_F R)], \tag{25}$$

where

$$M'(k_F R) = G^{2,1}_{2,4}\left(\begin{matrix} \frac{1}{2}, \frac{3}{2} \\ 1, 2, 0, \frac{-1}{2} \end{matrix} \middle| \ k_F^2 R^2\right) \tag{26}$$

and the undoped exchange interaction is

$$J^0_{AB}(\vec{R}) = \frac{3Ca^3}{R^3}\{1 + \cos[(\vec{K} - \vec{K}')\cdot\vec{R} + \pi - 2\theta_R]\}. \tag{27}$$

Similar to the previous subsection, we can use the asymptotic expansion of the Meijer G-Function in Eq. (25), $M'(k_F R)$, to find the long-distance behavior of $J_{AB}(\vec{R})$. Using the limit

$$\lim_{x\to\infty} M'(x) = \frac{3\pi - 10\cos(2x) - 8x\sin(2x)}{8\sqrt{\pi}x}, \tag{28}$$

the result is

$$\lim_{k_F R\to\infty} J_{AB}(\vec{R}) = \frac{J^0_{AB}(\vec{R})}{3\pi}[10\cos(2x_F) + 8x_F\sin(2x_F)]. \tag{29}$$

For short distance or small k_F, the appropriate limit is

$$\lim_{x\to 0} M'(x) = \frac{2x^2}{3\sqrt{\pi}}, \tag{30}$$

which leads to

$$\lim_{k_F R\to 0} J_{AB}(\vec{R}) = J^0_{AB}(\vec{R})[1 - \frac{16(k_F R)^3}{9\pi}]. \tag{31}$$

Short-distance behavior of $J_{AB}(\vec{R})$ can also be found using the asymptotic expansion of the Bessel functions for small arguments using Eq. (24).

Eqs. (15) and (25), which yield the RKKY interactions in the linear-band approximation and valid for all distances R, are two central equations of this paper. The computed results for J_{AA} and J_{AB} using these equations are shown in Fig. (2) and their long-distance forms are shown in Table I.

C. Moments on the bond centers and the beating of the RKKY interaction

For moments located on the bond center, the interaction is of the form $\mathcal{H}_{\rm int} = -\lambda\vec{S}\cdot\sum_p \vec{s}_p$, where the summation is over the two adjacent atoms. The exchange interaction becomes the sum of the site interactions:

$$J_{\rm bond}(\vec{R}) = 2J_{AA}(\vec{R}) + J_{BA}(\vec{R}) + J_{AB}(-\vec{R}). \tag{32}$$

Plugging in the values for the individual interactions from Eqs. (19) and (29), we get the result

$$\begin{aligned} J_{\rm bond}(\vec{R}) &= \frac{8C}{\pi(R/a)^3}\cdot\{2\cos(2k_F R) - \cos[(\vec{K}-\vec{K}')\cdot\vec{R}] \\ &\times [3\cos(2k_F R) + 4k_F R\sin(2k_F R)]\}. \end{aligned} \tag{33}$$

The resulting beating pattern of the RKKY interaction is shown in Fig. (4), which can be controlled by a gate voltage, which changes the Fermi momentum k_F, which in turn determines the period of the oscillations.

III. SUMMARY AND DISCUSSIONS

It has been demonstrated that the dopant carrier concentration in graphene can be controlled by a gate voltage or chemical doping.[22,23] This raises the interesting possibility of switching the magnetic interaction between ferro and antiferro. This is illustrated in Fig. 5, where the exchange interactions were evaluated using the full tight-binding bands as a function of k_F and the carrier density is given by $n = k_F^2/\pi$ in the linear-band region.

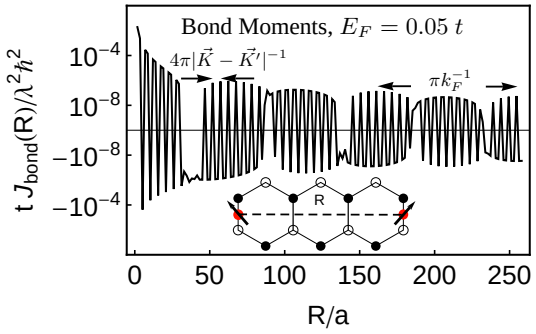

FIG. 4: (Color online) Beating pattern of the RKKY interaction for bond-centered moments separated along the zigzag direction.

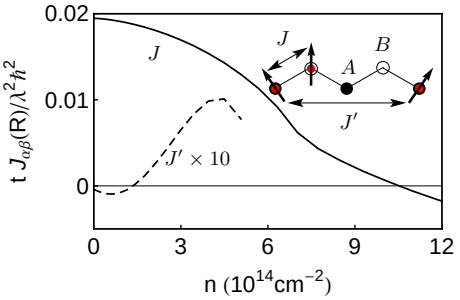

FIG. 5: (Color online) Switching the exchange interaction between ferro and antiferro by changing the carrier density in graphene with gate voltage. The larger the distance between the moments, the earlier is the switching, which is controlled by $k_F R$.

Now, a word on the magnitude of the RKKY coupling: If the itinerant and the localized spins were both on the same atom, then the exchange coupling λ is related to the Hund's-rule energy J_H, $\lambda\hbar^2 \simeq 2J_H \sim 2$ eV, so that for the maximum value of J shown in Fig. (5), the strength of the RKKY interaction $J\hbar^2 \simeq 30$ meV, which is large compared to the typical value ~ 5 meV in solids. For a magnetic atom located above the graphene plane, the RKKY interaction should be several times smaller, depending on the reduced value of λ.

Finally, we note that Table I is valid both for electrons and holes because of the particle-hole symmetry.[5] Mathematically, this follows from the fact that the net contribution to the susceptibility from a symmetric range of energy is zero as may be seen by taking the integral in Eq. (6) from $-\varepsilon$ to ε and by using the symmetry: $G^0_{\alpha\beta}(0,\vec{R},E) = G^0_{\beta\alpha}(\vec{R},0,E)$ and the fact that the product Im $G^0_{\alpha\beta}(0,\vec{R},E)\times$Re $G^0_{\alpha\beta}(0,\vec{R},E)$ is an odd function of energy.[18,20]

In summary, we provided analytical results for the RKKY interaction in graphene in the linear-band approximation and showed that these results agree with the numerical results obtained for the tight-binding bands if the Fermi momentum is small. The presence of the two characteristic momenta, viz., the Dirac cone momentum

$\vec{K} - \vec{K}'$ and the Fermi momentum k_F, leads to the unusual oscillatory features in graphene, different from the standard two-dimensional electron gas.

This work was supported by the U. S. Department of Energy through Grant No. DOE-FG02-00ER45818. We thank Jet Foncannon for helpful discussions on the Meijer G-functions.

[1] M. Sherafati and S. Satpathy, Phys. Rev. B **83**, 165425 (2011).
[2] M. A. Ruderman and C. Kittel, Phys. Rev. **96**, 99 (1954); T. Kasuya, Prog. Theor. Phys. **16**, 45 (1956); K. Yosida, Phys. Rev. **106**, 893 (1957).
[3] Y. Yafet, Phys. Rev. B **36**, 3948 (1987)
[4] B. Fischer and M. W. Klein, Phys. Rev. B **11**, 2025 (1975).
[5] S. Saremi, Phys. Rev. B **76**, 184430 (2007).
[6] L. Brey, H. A. Fertig and S. Das Sarma, Phys. Rev. Lett. **99**, 116802 (2007).
[7] M. A. H. Vozmediano, M. P. López-Sancho, T. Stauber and F. Guinea, Phys. Rev. B **72**, 155 121 (2005).
[8] V. K. Dugaev, V. I. Litvinov and J. Barnas Phys. Rev. B **74**, 224 438 (2006).
[9] J. E. Bunder and H.-H. Lin, Phys. Rev. B **80**, 153 414 (2009).
[10] A.M. Black-Schaffer, Phys. Rev. B **81**, 205416 (2010).
[11] S. R. Power and M. S. Ferreira, Phys. Rev. B **83**, 155 432 (2011).
[12] V. V. Cheianov and V. I. Fal'ko, Phys. Rev. Lett. **97**, 226801 (2006).
[13] B. Wunsch, T. Stauber, F. Sols and F. Guinea, New J. Phys. **8**, 318 (2006).
[14] C. Bena, Phys. Rev. Lett. **100**, 076601 (2008).
[15] Ádám Bácsi and Attila Virosztek, Phys. Rev. B **82**, 193405 (2010).
[16] J.-J. Zhu, D.-X. Yao, S.-C. Zhang, and K. Chang, Phys. Rev. Lett. **106**, 097201 (2011).
[17] B. R. K. Nanda and S. Satpathy, Phys. Rev. B **80**, 165 430 (2009).
[18] T. Horiguchi, J. Math. Phys. **13**, 1411 (1972).
[19] M. Sherafati and S. Satpathy, Phys. Stat. Solidi (B) (in press), arXiv:1103.4679.
[20] B. R. K. Nanda, M. Sherafati, Z. Popović, and S. Satpathy, arXiv:1105.1129
[21] C. S. Meijer, Nederl. Akad. Wetensch. Proc. Ser. A **49**, 344 (1946); Y. L. Luke, *The special functions and their approximations* (Academic Press, 1969), vol. 1, p. 171, 191, and 229; J. Fields, Math. Comput. **26**, 757 (1972).
[22] K. S. Novoselov, A. K. Geim, S. V. Morozov, D. Jiang, Y. Zhang, S. V. Dubonos, I. V. Grigorieva, and A. A. Firsov, Science, **306**, 666 (2004).
[23] J. L. McChesney *et al.*, Phys. Rev. Lett. **104**, 136803 (2010).